



Numerical Analysis of Mode-I Sif of an Arc Shaped Specimen Under Fatigue Loading and Comparison of Maximum Sif of Present Method with BCM.

Mahantesh S Matur, Iresh G Bhavi and Shashank Lingappa

EasyChair preprints are intended for rapid dissemination of research results and are integrated with the rest of EasyChair.

August 15, 2023

Numerical Analysis of Mode-I SIF of an Arc Shaped Specimen Under Fatigue Loading and Comparison of Maximum SIF of Present Method with BCM.

Mahantesh S Matur^{1*}, Iresh Bhavi², Shashank Lingappa³

¹ M. S. Ramaiah Institute of technology, Bangalore. Karnataka, India

² BLDEA's V.P.Dr.P.G.Halakatti College of Engineering and Technology, Vijayapur, Karnataka, India

³ Malnad College of Engineering, Hassan, Karnataka, India

^{1*}E-mail:mahanmatur@msrit.edu

Abstract

Practically, high risk products like nuclear plant steam generators, thick cylinders etc. do fail either by Mode-I or Mode-II or Mode-III. Mode- I failures are more and hence studied about the same very often. Root cause of most of these products are the presence of inbuilt or in-service flaws in the structures. Although designers give more importance to design featuring, notches and grooves to minimize the stress, fatigue failures of the components repeatedly take place during the service in the industries. Hence it is necessary to understand the mechanism of Fatigue crack growth (FCG) in metals through the tests using the suitable experimental setup. After vigorous literature survey, it is noticed that, an Arc shaped Tension specimen (AT) can be used as it is very useful for testing the properties of thick wall pipes.

To meet the set objectives, present work is begin with FCG testing of AT specimen of Al alloy using the Experimental setup. Stress Intensity Factor(SIF) range, number of fatigue cycles are recorded and Paris' constants are determined. To study the effect of Mode-I loading on the SIF at the crack tip, an AT specimen with 2 crack geometries, i.e crack on inner surface and outer surface are considered independently. In both the cases, same radius ratio and crack size of the specimen is maintained. To execute fatigue load, maximum and minimum loads so obtained from the experimental study is used in Finite Element analysis (FEA). AT specimen with 1mm inner surface crack is modeled and SIF is evaluated. The process is continued in a step of 1mm crack length increment, up to the stage when maximum SIF reaches the critical value of the material. Using the Paris' constants, FCG rate is computed. Number of stress cycle is calculated using the integral formula. The outcome in terms of relative crack length vs maximum SIF as obtained by the present method is compared with Boundary Collocation Method (BCM) results of literature. Deviation in the maximum SIF of 2% and 9.49% between the present method and BCM results is observed for inner and outer crack respectively.

Also, it is been observed that, stress required to widen the crack at the inner surface of the specimen is more than the stress required to widen the crack at the outer surface. Al alloy can sustain more number of fatigue cycles, if the crack is at the outer surface than the crack at inner surface under the similar mode of loading. This is due to the fact that, as outer crack induces comparatively less stress gradient and thus crack can extend to larger size before reaching to the unstable growth.

Key points: Arc shaped Tension specimen, Fatigue crack growth, Stress Intensity Factor, Finite Element analysis.

1. Introduction

In designing structural or machine components, an important step is the identification of the most likely mode of failure and the application of a suitable failure criterion. Three modes of failure namely Mode-I, called as opening mode, Mode-II called as sliding mode and Mode-III called as tearing mode were identified. Practically, material may fail in one of these failure modes and out of these, Mode-I failures are more and hence studied about the same very often. Numerous investigations performed by many authors shows that, the slow crack propagation mechanism that causes the majority of pipe failures can be simulated in the laboratory using different commercial software. These studies included the failure of components either under structural load during the service or with creep at elevated temperatures. Wherein, variable load or fatigue load is a repetitive load due to which material will fail without any prior indication. Hence fatigue failure depends on many factors like, mean stress, stress amplitude, number of cycles, stress concentration [1], residual stress [2], strain hardening and creep [3]. Varieties of cracks have been observed in the components because of wrong methods of manufacturing practices. Few examples are surface cracks, embedded cracks and edge cracks. In case of small cracks such as kinks and bifurcation of cracks at grain boundaries, which is in the order of several grain diameters, SIF is affected by various factors caused by grain size.

The reviewed paper illustrates that [4], when crack runs along the grain boundaries, it is not straight, but oriented by different angles. The paper concludes with key observation as, for the accurate prediction of the crack growth in a structure, SIF should be evaluated, based on the realistic assumptions of crack shape and stress distribution. Key issue out of these factor is the influence of curved surface or the difficulty associated with the geometrical parameters on the design of vessels that make the structural integrity very cumbersome. For example, under the action of internal pressure there exist a high stress concentration factor at the nozzle inner corner, as the nozzle is connected with pressure vessel. With the increasing use of pipes, high pressure-cylinders, boilers and many types of equipment of curved surfaces, there is huge requirement of correct assessing methods and sufficient structural integrity in these components for longer periods of usage.

Hence the present study begins with the fabrication of an, AT specimen as recommended by ASTM E-399 [5] using the wire EDM method. All AT specimens made up of Al alloy are subjected to FCG test, as recommended by ASTM E647 using the fatigue testing machine independently [6]. SIF values with crack length are generated and later tabulated to calculate Paris' constants. The number of fatigue cycles required before failure of the material are recorded for further comparison. It is quite important to note that, study of low cycle fatigue gained more attentions, as an excellent prediction results were observed for crack below the 10^5 cycles [7].

To study the effect of Mode-I loading on the SIF at the crack tip, an AT specimen with 2 crack geometries i.e. crack on inner surface and outer surface are considered independently (Fig. 1). To prevail Mode-I failure, inner surface crack geometry is subjected to tensile load while in the separate study, the outer surface crack geometry is subjected to compressive load. In both the cases, same radius ratio and crack size of the specimen is maintained. To execute fatigue load, a maximum load of 3300 N and minimum load of 990 N are applied independently for the evaluation of $(K_I)_{max}$ and $(K_I)_{min}$. An Al alloy specimen with 1 mm inner surface crack length is considered initially and SIF is evaluated using the Ansys software. The process is continued in a step of 1 mm crack length increment, up to the stage when $(K_I)_{max}$ reaches K_{IC} , the critical SIF. Using the

maximum and minimum SIF, stress intensity range is calculated for each crack length. Using the Paris' constants, i.e. C & m so obtained from the experiments, FCG rate is computed. The number of stress cycles is calculated using the integral form, i.e.

$$N = \int_{a_i}^{a_f} \frac{da}{C(\Delta K)^m} \quad (1)$$

The outcome in terms of relative crack length vs. maximum SIF as obtained by present method is compared with the BCM results of literature [8]. Minimum deviation in the maximum SIF between the present method and BCM results is observed for specimens with inner and outer crack respectively. Finally the present work is concluded with a good number of key observations, distinguished features and critical aspects related to crack growth on the curved surface geometry under mechanical loading.

2. Experimental study

In this section brief explanation regarding the material, specimen geometry and test method employed in studying the FCG behavior of Al alloy in the presence of notch is presented.

2.1 Material and Specimen details

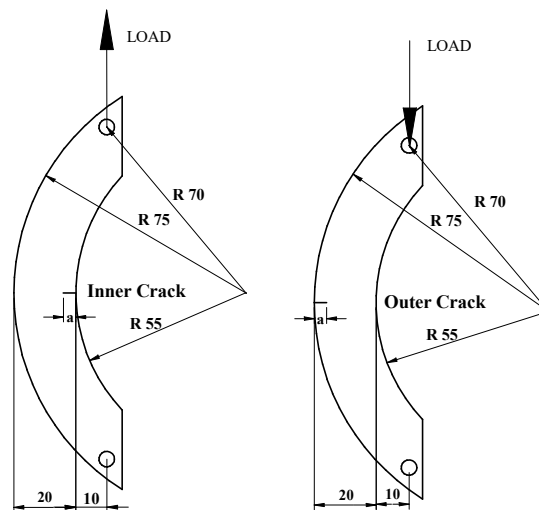


Figure 1. Arc Shaped Tension Specimen with Surface Cracks

Most of the investigative studies were carried, considering either steel or Al alloys, as these two materials are the most dominating among the metals in the present situation. Al alloy 6061 is heat treatable extruded alloy with medium to high strength capabilities. Typical applications for Al alloy 6061 include: Aircraft and aerospace components, marine fittings, transport, bicycle frames, driveshaft, etc. Specimen raw material is extruded bar of 160mm diameter and length 150 mm. An arc shaped tension specimen as shown in figure 1 (with inner crack only) is produced from the bar following different conventional machining operations. Wire EDM is used for machining critical part of the specimen. During the wire EDM process, the wire carries one side of an electrical charge and the specimen carries the other side of the charge. When the wire gets close to the specimen, due to the attraction of electrical charges a controlled spark is created, which later melts and vaporizes the microscopic sizes of material.

The spark also removes a chunk of the wire and automatically advances new wire for the next sequence of operation. Machining parameters of this machine is as shown in Table

1. Initially, using wire EDM, ring shaped raw pieces are cut into two pieces, later notch is created on the inner surface of 4mm length and 0.25 mm radius. With maximum care clip gauge holding grip at the notch is created with wire EDM as per the dimensions suggested the ASTM standard. All the specimens were fabricated with maximum care in order to meet the standards, so that scatter in the test results would be as minimum as possible.

Table.1 Machining Parameters Selection

Machining method	Details of operation	Selection parameters
Wire EDM	Wire diameter range	: 0.1 – 0.3 mm
	Wire material	: Brass
	Electrolyte used	: Deionised water
	Wire speed	: 2×10^{-3} mm / sec
	Machine power	: 20 Hp
	Software used	: Auto Cad 2004

2.2 Test Method:

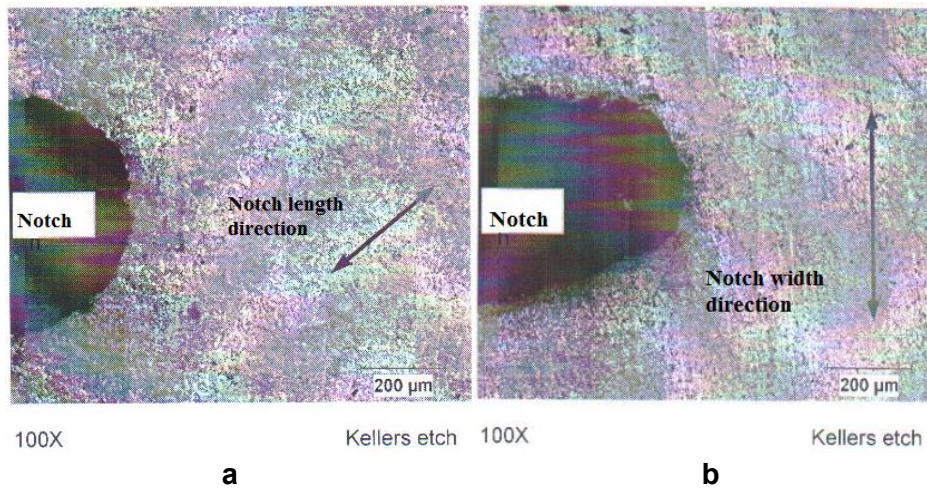


Figure 2. Specimens Under Microscope, Showing Notch Along a) Length Direction b) Width Direction

Optical Metallurgical microscope is used to examine the round shape of the notch that is cut in the AT specimens using wire EDM and also check if any initial cracks of major size at the nose end of the notch. Figure 2a and 2 b, shows the same respectively. FCG test is carried out using the facilities as highlighted in figure 3. As the fatigue load is under taken, the load ratio of 0.3 and load range of 2.31 kN is applied, at room temperature. Loading is continued till the specimen fails. Then the clip gauge is dismantled and the failed specimen is unloaded and preserved for further comparison. Figure 4. shows the fatigue failure pattern of Al-alloy specimen with inner surface notch.



Figure 3. Fatigue Testing Machine

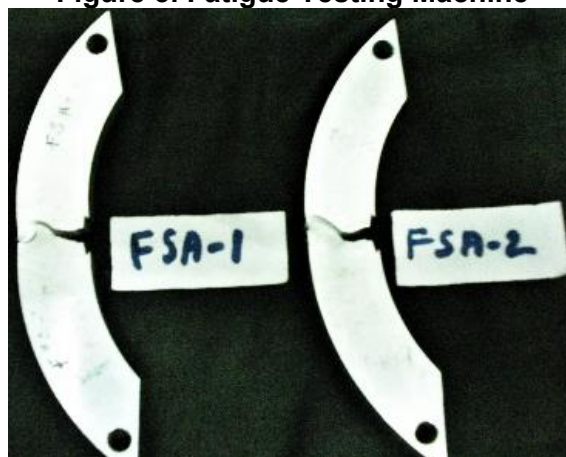


Figure 4. Failed Al-Alloy Specimens Under Fatigue Load

3. Results and Discussion

The experimental results in terms of number of stress cycles vs crack length were recorded and plotted as shown in Figure 5. There is a gradual increase in crack length with increase in stress is observed.

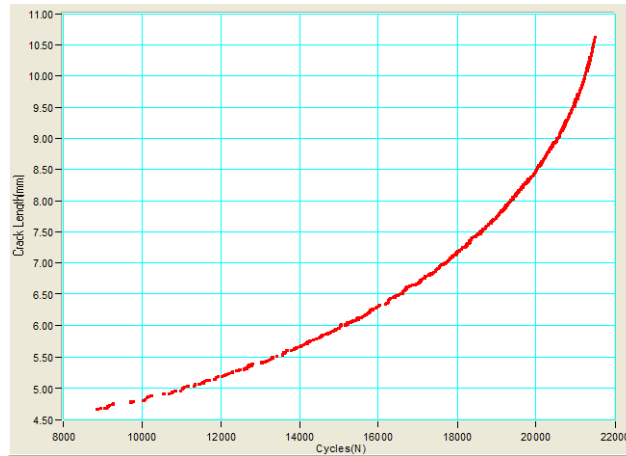
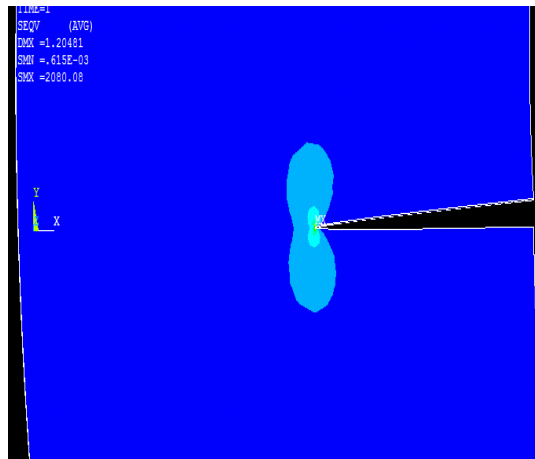


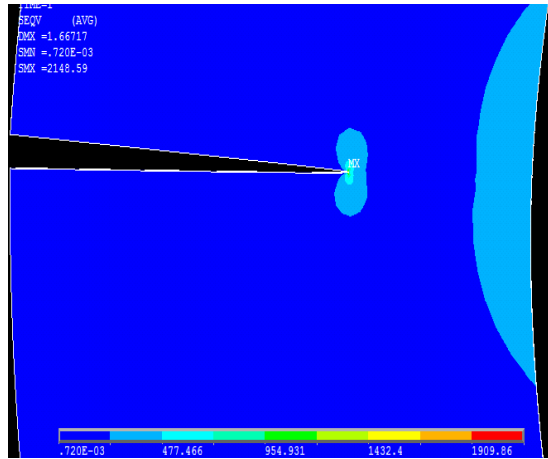
Figure 5. Experimental Result of Cycles vs Crack Length for Al Alloy

3.1 Finite Element analysis of Inner surface crack

Aluminum specimen with surface crack is considered, separately for inner and outer surfaces. A finite element analysis is carried out, keeping all the factors constant, except the loading direction. Initially, 1 mm inner surface crack length is created and SIF is evaluated. The nodal solution thus obtained provides the maximum stress is obtained at the tip of a crack as shown in fig. 6. Crack length 2 mm is created separately and analysis process is continued. At 8.5 mm crack length, $K_{I \max}$ researches K_{IC} , the critical SIF. Similarly, SIF evaluation process is repeated for minimum load to obtain minimum SIF. Table 2. shows the stress intensity range recorded for the specimen. Using the Paris constants so obtained from the experiments, FCG rate is computed. Table 2. gives the details of crack growth rate over the increase in crack length. The number of cycles up to the failure is calculated using the integral form, equation 1. Table 3 shows the total life cycle of the specimen under consideration.



a



b

Figure. 6 Von Mises Stress Distribution Around the Crack Tip for a) Inner Crack b) Outer Crack

Table 2. Stress Intensity Range and Crack Growth Rate for Inner Crack

Crack length, mm	Kmax (MPa√m)	Kmin (MPa√m)	ΔK (MPa√m)	da/dn (Crack growth rate)
1	7.14	2.14	5.00	1.15E-05
2	10.14	3.03	7.11	3.51E-05
3	12.48	3.73	8.74	6.76E-05
4	13.95	4.19	9.76	9.60E-05
5	16.98	5.09	11.88	1.79E-04
6	19.47	5.84	13.62	2.76E-04
7	22.28	6.68	15.60	4.24E-04
8	25.67	7.56	18.12	6.81E-04
8.5	27.66	8.30	19.36	8.41E-04

Table.3 Number of Stress Cycle for Inner Crack Geometry

Initial crack length	final crack length	crack growth	Number of stress cycles	total number of cycles
0	1	1	86957	86957
1	2	1	28490	115447
2	3	1	14793	130240
3	4	1	10417	140657
4	5	1	5587	146244
5	6	1	3624	149868

6	7	1	2359	152227
7	8	1	1468	153695
8	8.5	0.5	594	154289

3.2 Finite element analysis of Outer surface crack;

In order to promote Mode-I failure of the specimen, an outer crack of same length, is considered and subjected to the same load in reverse direction. The procedure adopted in bringing the results for inner surface cracks are repeated for outer crack also. Figure 6b shows the Von Mises distribution. Table 4. shows the stress intensity range thus recorded for the specimen. Using the Paris constants, FCG rate is computed and table 4. gives the details of crack growth rate over the increase in crack length. The number of cycles up to the failure is calculated using the integral form as discussed early. Table 5 gives the total life cycle of the specimen under consideration.

Table 4. Stress Intensity Range and Crack Growth Rate for Outer Crack

Crack length,mm	K _I max Mpa √m	K _I min Mpa √m	ΔK in Mpa √m	da/dn (Crack growth rate)
1	6.55	2.01	4.54	8.48E-06
2	7.21	2.16	5.05	1.19E-05
3	8.39	2.52	5.88	1.92E-05
4	9.57	2.87	6.70	2.91E-05
5	10.82	3.26	7.56	4.27E-05
6	12.35	3.64	8.71	6.68E-05
7	13.88	4.11	9.77	9.61E-05
8	15.69	4.60	11.09	1.44E-04
9	17.88	5.35	12.53	2.12E-04
10	20.03	6.01	14.02	3.02E-04
11	23.87	7.29	16.58	5.15E-04
12	27.83	8.35	19.48	8.57E-04

Table.5. Number of Stress Cycles for Outer Crack Geometry

Initial crack length	final crack length	crack growth	Number of stress cycles	total number of cycles
0	1	1	117976	117976
1	2	1	84199	202174
2	3	1	52099	254274
3	4	1	34418	288692
4	5	1	23404	312096
5	6	1	14967	327063
6	7	1	10403	337466
7	8	1	6964	344430

8	9	1	4720	349149
9	10	1	3308	352457
10	11	1	1944	354400
11	12	1	1167	355567

3.2 Discussion-1; Crack length Vs stress intensity range

A single parameter, that characterizes the whole stress field at the crack tip, is Stress intensity factor, K . In addition to the usual dependence on crack length a , SIF for arc-shaped specimens also depends on the position of the loading ($x/W=0.5$) and on the radius ratio of the specimen (R_o/R_i).

Let,

F = Applied load

X = Horizontal distance of edge of the crack from loading line in case of inner surface crack

x' = Horizontal distance of edge of the crack from loading line in case of outer surface crack

b = Vertical distance of edge of the crack from loading line

F_y and F_y' = Localized load components at crack in case of inner and outer crack respectively

W = Width of the specimen

$N.A_i$, $N.A_o$ = Neutral axis for inner crack and outer crack specimen

$\frac{R_o}{R_i}$ = Ratio of outer to inner radius of the specimen = 1.36

Γ_p , Γ_m = Stress intensity coefficients for load P and moment M . [Ref.1]

σ_p , σ_m = Stress due to direct load, P and moment, M .

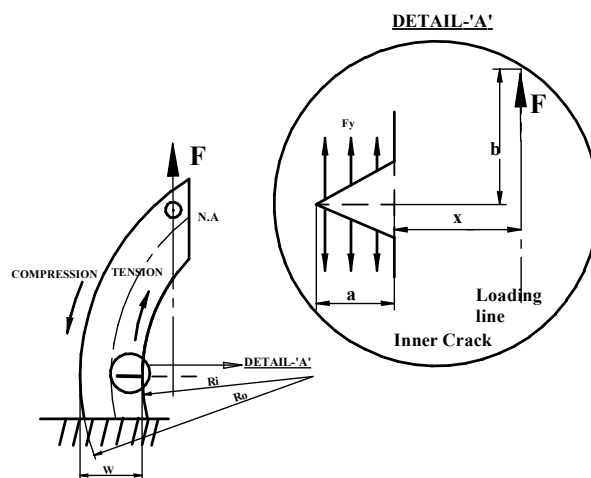


Figure 7. Mode-I Loading for Inner Surface Crack

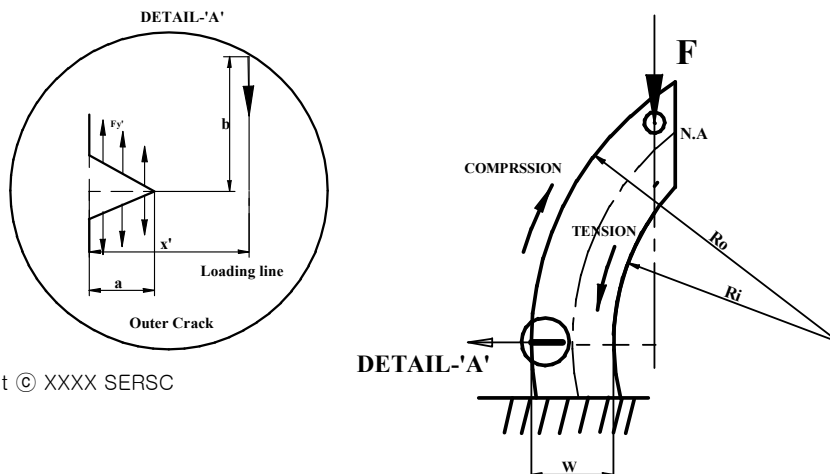


Figure 8. Mode-I Loading for Outer Surface Crack

There will be two stress components, namely stress due to direct load and stress due to bending moment. It follows that, for the inner crack specimen with applied load F , the widening of the crack requires, a sufficiently more localized force components at and around the crack and it is equal to F_y . In the similar manner, the widening of the outer crack happens by sufficiently more localized force components of F_y' as shown in fig 7 & 8. As the load acts at a distance from the edge of the crack, there is a moment induced due to eccentricity. The moment induced due to force F_y and F_y' will be different as the values of x and x' will differ for inner and outer cracks respectively. Attempt has been made, in this context, to compare the SIF obtained through the use of BCM by the author with the present method and is as mentioned below.

Review of the Paper;

In the literature[8] the importance of C.G of the uncracked segment of the specimen, is deliberated, while calculating the moment due to force applied on the C- specimen. Author has used BCM to get deferent set of Stress Intensity coefficients, in order to obtain the maximum SIF at the crack tip. Table 7 & 8 gives the same with SIF comparison. As in the literature[8], radius ratio of 1.33 was not available, the average of 1.1 and 1.5 were considered for the SIF calculation. Fig. 9 & 10 gives the maximum SIF by the BCM well fit with the present method. Increase in stress intensity with increase in crack length is observed in both the cases. It is clear that, stress required to widen the crack to larger size at the inner surface of the specimen is more than the stress required to widen the crack at the outer surface. From Table. 7, for inner cracked specimen, the average error in the maximum SIF obtained by using FEM and the SIF results, by BCM is less than 2%. In case of outer crack also, SIF is increasing with the crack length. It is observed that, deviation of 9.5% in the maximum SIF results for outer cracked specimen, between present and BCM.

Table.7 Max SIF Comparison for Inner Crack

Crack length, mm	a/W	Γ_p	σ_p	Γ_m	σ_m	[KI] _{BCM}	[KI] _{present}	% Error
2	0.1	1.468	18.33	1.679	128.3	325	320	1.54
4	0.2	1.126	20.62	1.393	170.15	465	441	5.16
6	0.3	0.9125	23.57	1.201	232.4	616	615	0.16
8	0.4	0.778	27.5	1.061	330	813	811	0.25

Table.8 Max SIF Comparison for Outer Crack

Crack length, mm	a/W	Γ_p	σ_p	Γ_m	σ_m	[KI] _{BCM}	[KI] _{present}	% Error
2	0.1	1.484	18.33	1.504	116.11	270.78	228.13	15.75
4	0.2	1.206	20.62	1.286	139.21	364.7	302.52	17.05
6	0.3	1.013	23.57	1.132	171.73	447	390.37	12.67
8	0.4	0.8725	27.50	1.013	220.00	540	496.1	8.13
10	0.5	0.767	33.00	0.921	297.00	668	633.38	5.18

12	0.6	0.689	41.25	0.846	433.00	864	879.85	-1.83
----	-----	-------	-------	-------	--------	-----	--------	-------

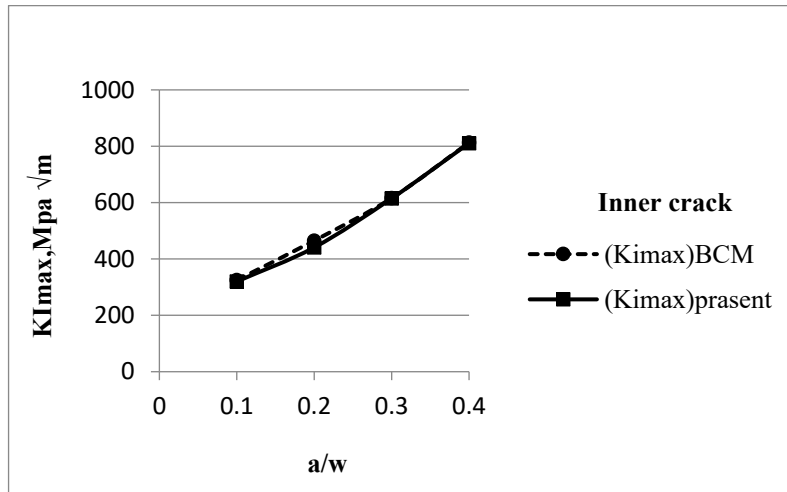


Figure 9. Comparison of Max SIF with BCM Results for Inner Crack

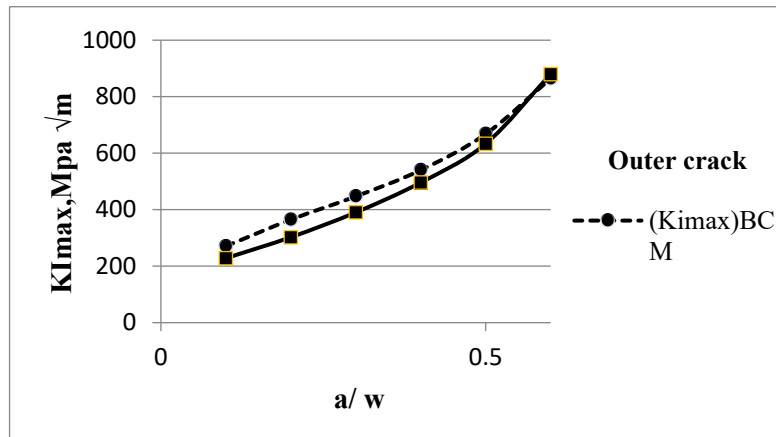


Figure 10. Comparison of Max SIF with BCM Results for Outer Crack

It is observed that, in case of inner cracked specimen, material near the inner surface experience the tension where as material near the outer surface experience the compression. A reverse mechanism occurs in case of outer cracked specimen. Position of the neutral axis will effect the stress environment at the crack tip severely and it is proved to be correct as per the results obtained in the present study.

4 Conclusion

Investigation of crack growth on the inner and outer surface of arc shaped specimen were carried out. Conclusion of the present work could be drawn as below; From the numerical investigation, maximum bending stress is observed for inner surface crack than that of the outer surface crack under identical loading condition. This attribute of boundary stress distribution, increases the SIF for an inner cracked specimen, but suppresses it when the specimen is externally cracked. This behavioral aspect may takes place when no other factor such as residual stress, environment, surface finish, etc. has a stronger counter effect. More number of fatigue cycles can be withstand by the external surface crack than the

internal surface crack under the similar mode of loading. As, external crack induces comparatively less stress gradient and thus crack can extend to larger size before reaching to unstable growth.

Acknowledgments

I sincerely express my gratitude to my guide Dr. V. Krishnan and my college for providing the opportunity to carry the present work.

References

- [1] Andrea. Carpinteri, 'Notched double curvature shells with cracks under pulsating internal pressure', International Journal of Pressure vessels and Piping, 86(2009), pp. 443-453.
- [2] Jerome Isselin and Tetsuo Shoji, 'Crack initiation resistance characterization of weld by small punch test in boiling water reactor environment', International Journal of Pressure vessels and Piping, 93-94 (2012), pp. 22-28.
- [3] P.J. Holt and R. A. W. Bradford, 'Application of probabilistic modelling to the life time management of nuclear Boilers in the creep regime: Part 1', International Journal of Pressure vessels and Piping, 95 (2012), pp. 48-55.
- [4] Cotterell. B. and Rice. J. R , 'Slightly curved or Kinked Cracks', International Journal of Fracture, 16(1980), pp-155-169.
- [5] ASTM:E 399-90(Reapproved 1997), Standard test method for Plane –strain Fracture Toughness of Metallic Materials, American Society for Testing and Materials; 2003.
- [6] ASTM:E647, FCG Testing Standard, American Society for Testing and Materials; 2006-10.
- [7] S. M. Beden, 'Review of fatigue crack propagation models for Metallic components', European Journal of Scientific Research, ISSN 1450-216X Vol.28, No.3(2009), pp.364-397.
- [8] Bernard. Gross and John E. Srawley, 'Analysis of radially cracked ring segments subject to forces and couples', Development in Fracture Mechanics Test Methods Standardization , ASTM STP 632,W.F.Brown, Jr., and J. G. Kaufman, Eds., ASTM, 1977,pp.39-56.



Mahantesh S Matur, M.S.Ramaiah institute of Technology, Bangalore, Karnataka, India.



Iresh Bhavi, BLDEA's V.P.Dr.P.G.Halakatti College of Engineering and Technology, Vijayapur , Karnataka, India



Shashank Lingappa, Malnad College of Engineering, Hassan, Karnataka, India.